

Article

Bright High-Order Harmonic Generation around 30 nm Using Hundred-Terawatt-Level Laser System for Seeding Full Coherent XFEL

Luyao Zhang, Yinghui Zheng *, Guicun Li, Zhengmao Jia, Yanyan Li, Yi Xu, Yuxin Leng, Zhinan Zeng *, Ruxin Li and Zhizhan Xu

State Key Laboratory of High Field Laser Physics, Shanghai Institute of Optics and Fine Mechanics, Chinese Academy of Sciences, Shanghai 201800, China; zhangluyao@siom.ac.cn (L.Z.); lgccst@siom.ac.cn (G.L.); jiazhengmao@siom.ac.cn (Z.J.); yyli@siom.ac.cn (Y.L.); xuyi@siom.ac.cn (Y.X.); lengyuxin@mail.siom.ac.cn (Y.L.); ruxinli@mail.shcnc.ac.cn (R.L.); zzzxu@mail.shcnc.ac.cn (Z.X.)

* Correspondence: yhzhang@siom.ac.cn (Y.Z.); zhinan_zeng@mail.siom.ac.cn (Z.Z.)

Received: 20 July 2018; Accepted: 20 August 2018; Published: 24 August 2018



Featured Application: The main application of this work is to produce high-energy high harmonic generation (HHG) as a seed of soft X-ray free-electron laser. Furthermore, it has some practical applications, such as extreme-ultraviolet (XUV) pump-probe spectroscopy, intense attosecond pulse generation, and XUV lithography.

Abstract: In the past few years, the laser wakefield acceleration (LWFA) electron is a hot topic. One of its applications is to produce soft X-ray free-electron laser (XFEL). During this process, high harmonic generation (HHG) is a potential seed. To decrease the timing jitter between LWFA and HHG, it is better for them to come from the same laser source. We have experimentally investigated bright high-order harmonic generation with a 200-terawatt (TW)/1-Hz Ti: Sapphire laser system. By using the loosely focused method and optimizing the phase-matching conditions, we have obtained bright high-order harmonics around 30 nm. Output energy of the 29th harmonic (27.6 nm) reaches as high as 100 nJ per pulse, and the harmonic beam divergence is estimated to be 0.3 mrad in a full width at half maximum (FWHM). Although the hundred-TW-level laser system has the problems of poor beam quality and shot-to-shot energy fluctuation for HHG, the generated soft X-ray (~30 nm) sources can also have good stability by carefully optimizing the laser system.

Keywords: high-harmonic generation; terawatt-level laser system; XFEL

1. Introduction

High-order harmonic generation (HHG), a highly nonlinear interaction of light with matter, has been extensively used for producing coherent extreme-ultraviolet (XUV) or X-ray light sources [1–3]. Compared with other XUV light sources, such as free-electron lasers (FELs), X-ray lasers (XRLs) and synchrotron orbit radiation (SOR), HHG has many excellent features, such as high peak intensity, full coherence, ultrashort pulse duration, wide tunability, and tabletop configurations. However, the generated harmonics are generally weak because the HHG process is highly nonlinear and non-perturbative [4], which will limit practical applications, such as XUV pump-probe spectroscopy [5], intense attosecond pulse generation [6], XUV lithography [7] and FEL seeding [8,9].

Therefore, up to now, many groups have devoted themselves to increasing the conversion efficiency (CE) and the pulse energy of HHG. Ditmire et al. [10] tried to change a lot of parameters, including driving laser wavelength, focal geometry, and peak intensity in the experiment, and obtained individual harmonics with energies as high as 60 nJ at wavelengths as short as 20 nm, but the CE

was only 10^{-7} . Further, E. Constant et al. [11] optimized the medium length for harmonics generation by considering reabsorption, and the CE was increased to 4×10^{-5} . Moreover, by using the loosely focused method under the phase-matching condition, E. Takahashi et al. obtained the HHG of 0.3 μJ at the 27th harmonic (29.6 nm) in Ar [12], 4.7 μJ at the 13th harmonic (62 nm) in Xe [13], and 50 nJ at the 59th harmonic (13.5 nm) in Ne [14]. Based on these energy scaling methods, C. Erny et al. [15] performed a detailed metrology of high-order harmonics and the generated XUV output was good enough for FEL seeding.

However, all these previously reported results are based on less than a few terawatt (TW) driving laser system with high repetition rates, such as dozens or even a thousand of hertz, which limits the application of HHG to some extent. For example, generation of fully coherent X-ray free-electron laser (XFEL) by using laser wakefield acceleration (LWFA) and HHG seeding is currently a popular research field. The benefit of the seeding is amazing, including reducing the timing jitter of the emission from the FEL, reducing the size of the FEL for a saturated amplification and improving coherence. On the other hand, the limitation of photon number of a high harmonic source no longer exists, which is quite important for many potential applications. Based on a home-made 200-TW/1-Hz Ti: Sapphire laser facility [16], significant progress on LWFA has been achieved in Shanghai Institute of Optics and Fine Mechanics (SIOM) [17]. The progress on LWFA has also opened a new opportunity for the development of compact XFEL. Researches on full-coherent HHG-seeding XFEL are now carrying out at SIOM. However, producing XFEL requires at least multi-hundred-TW laser systems. To decrease the timing jitter between LWFA and HHG, it is better for them to come from the same laser source. However, the beam quality, and the shot-to-shot energy fluctuation of the hundred-TW-level laser are not comparable to a few TW laser system, and they are still problems for HHG. Thus, it is a promising work to optimize HHG driven by multi-hundred TW laser systems.

In this work, we used a 200-TW/1-Hz Ti: Sapphire laser amplifier system based on a chirped pulse amplification [16]. This laser system consists of four-stage Ti: Sapphire amplifiers, which can produce an output energy of 8 J at a central wavelength of 800 nm with a pulse duration of 30 fs (FWHM). In order to achieve the full-coherent XFEL, the laser was separated into two beams. The main laser beam, which has a peak power of nearly 200 TW, was used to produce the high-performance electron beam by LWFA. The other laser beam, which has a peak power of 1.3 TW, was used to produce soft X-rays in the HHG experiment. By using generally adopted loosely focusing method and optimizing the phase-matching conditions, we have obtained bright high-order harmonics around 30 nm. Output energy of the 29th harmonic (27.6 nm) reached as high as 100 nJ per pulse, and the harmonic beam divergence was estimated to be 0.3 mrad (FWHM). In this experiment, bright stable HHG has been achieved, which is an important step in the production of highly stabilized ultrashort XFEL.

2. Materials and Methods

The experimental setup of HHG is shown in Figure 1. The infrared (IR) laser beam, which has a diameter of 40 mm, is adjusted by a diaphragm with a diameter of approximately 17 mm, and loosely focused by a plano-convex lens, which has a focal length of approximately 5000 mm and is mounted on a motorized translation stage. The spot diameter around the laser focus had been measured to be $\sim 300 \mu\text{m}$ and the confocal parameter $b = 2z_R \approx 180 \text{ mm}$, where z_R is the Rayleigh length. Then, the focused IR pulse is guided into the target chamber through a CaF_2 window mounted at the Brewster's angle of the IR pulses to avoid light reflection, and interacted with the argon gas in a gas cell that is located around the laser focus. The length of the gas cell can be adjusted from 0 to 150 mm. The generated harmonics, propagating with the residual IR pulses, subsequently pass through an iris diaphragm (a diameter, $\sim 4 \text{ mm}$), which partially blocks the IR pulses, and then are delivered into the measuring section.

In the measuring section, a gold-coated spherical mirror (SM), mounted on a motorized translation stage is used to send the XUV beam either into the flat-field grating spectrometer equipped with an XUV charge-coupled device (XUV-CCD, Andor iKon-L, Oxford Instruments plc, Abingdon, UK) camera for

spectral measurement or into an XUV photodiode detector (AXUV100G, Opto Diode Corp, Camarillo, CA, USA) for absolute energy measurement. Specifically, when the SM is inserted into the beam path, the harmonics are reflected by the SM, passing through a slit, and then diffracted by a flat-field grating. The spectrally resolved far-field high-order harmonics are detected by the XUV-CCD camera. On the other hand, when the SM is removed from the beam path, the harmonics are directly reflected by the silicon mirrors, and then illuminating the photodiode detector.

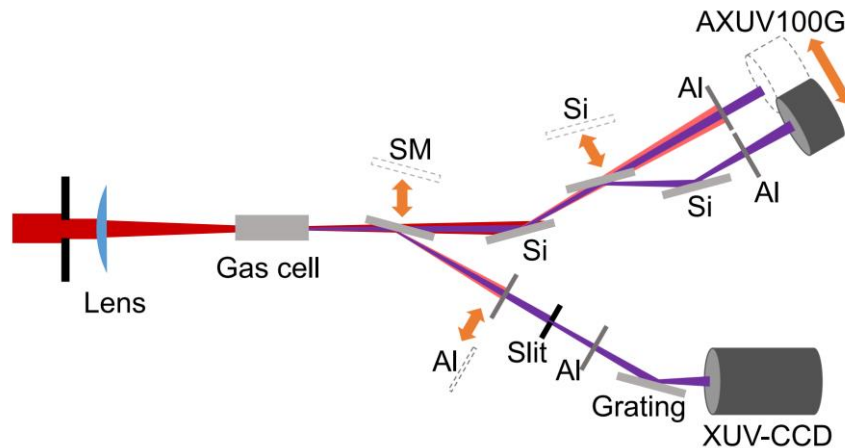


Figure 1. Schematic of the experimental high-order harmonic generation (HHG) setup. Spherical mirror (SM): gold-coated spherical mirror; Al: 500 nm-thick aluminum filters; Si: silicon reflecting mirror. The equipment marked with a double-headed arrow is mounted on the motorized translation stage.

3. Results

We used the pulse energy of only ~17 mJ in this experiment, because the CaF₂ windows affect the frequency spectrum of the pump pulse greatly if the pulse energy is higher. Owing to the loss from multiple cutout of the center beam and other optical elements, the final peak power of driving laser for HHG was about 0.57 TW. The intensity at the focus point was 8×10^{14} W/cm². Ar gas was filled in the gas cell with a 100-mm medium length. Figure 2 presents the intensities of the 29th harmonic with respect to various pressures in the gas cell and the relative positions between the laser focus and the gas cell, respectively. Obviously, the intensity of the 29th harmonic reached the maximum around the pressure of 12 Torr and the relative position was 0 mm, which is the optimized phase-matching condition.

Figure 3 shows the harmonic spectra in the optimized phase-matching condition. These harmonics were accumulated with 10 shots and only one Al filter in the beam path. It is worth noting that the other filter was mounted on a motorized translation stage. By comparing the harmonic spectra detected with one filter or two, we could obtain the transmission ratios of the aluminum filters for individual harmonics. We did not use the transmission ratio in a database, because the transmission ratio of the Al filter can gradually change due to oxidation. By using this method, we estimated the transmission ratio of a 500 nm-thick aluminum filter was 5% for the 29th harmonic.

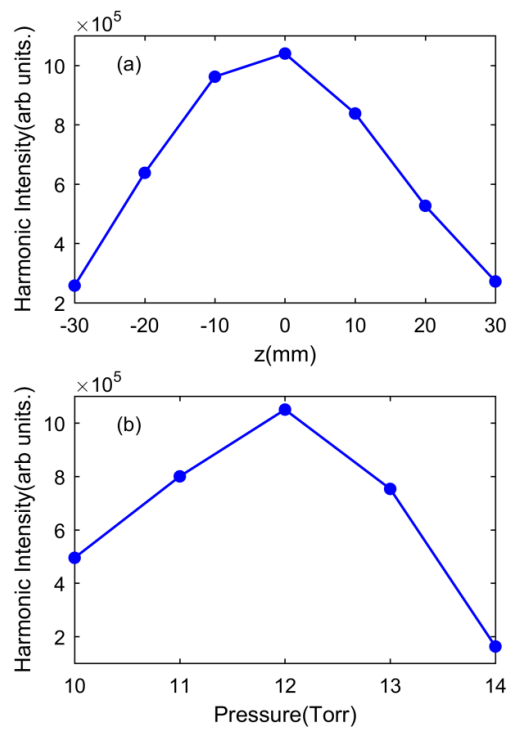


Figure 2. The 29th harmonic intensity obtained in the experiment. (a) Intensity of the 29th harmonic as a function of the relative position between the laser focus and the gas cell; (b) intensity of the 29th harmonic as a function of the pressure in the gas cell.

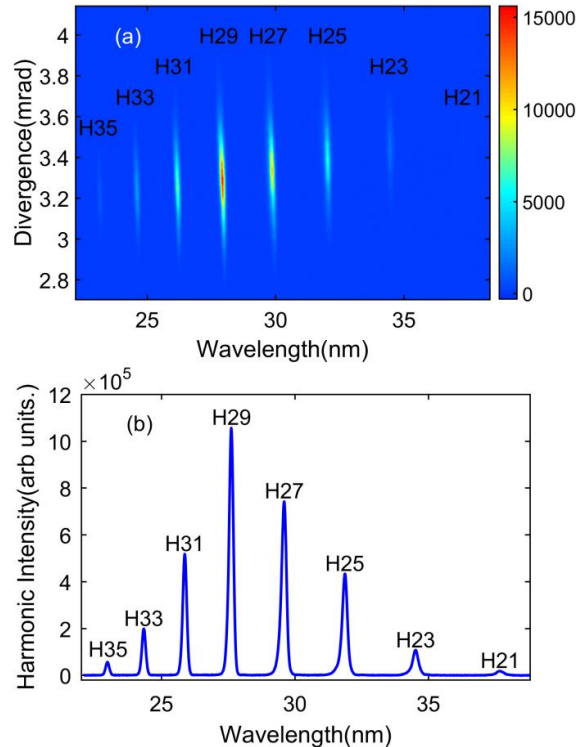


Figure 3. Measured harmonics in a 100-mm medium length with Ar gas. (a) Spatial (y-axis) and spectral (x-axis) profiles of HHG in the optimized conditions. (b) Spatial integration of HHG in the optimized condition.

When the SM is removed from the beam path, the harmonics illuminate the photodiode detector for the absolute output energy measurement. Here, three Si mirrors were mounted at the Brewster's angle of 75° (light grazing incidence angle, $\sim 15^\circ$), acting as beam splitters that can efficiently reflect the harmonics, but absorb most of the fundamental pulses. E. J. Takahashi et al. [18] has determined that the reflectivity of Si mirror is ~ 0.56 for a 30-nm spectral region, when it is at the Brewster's angle for 800 nm. In this section, the IR pulses were completely blocked, and only the remaining XUV signal was sent into the photodiode detector (AXUV100G). By comparing the HHG energy obtained with one or three Si mirrors, the measured reflectivity of a Si mirror was 0.42, lower than that measured by E. J. Takahashi et al. [18], which might be influenced by the roughness of Si mirrors.

Thus, the obtained total energy of HHG was estimated to be ~ 300 nJ/pulse in the optimized phase-matching condition. Considering the spectral distribution in Figure 3b, every individual harmonic energy was separately calculated. Therefore, the 29th harmonic energy was estimated to be ~ 100 nJ by a single shot.

By considering the distance between the gas cell and the XUV-CCD camera, the spatial profile of harmonics was converted to the emission angles. The spatial profile of the 29th harmonic in the optimized condition is shown in Figure 4. The 29th harmonic beam divergence was estimated to be ~ 0.3 mrad (FWHM).

We did not measure the pulse duration of the harmonic. Because the laser repetition is very low, only 1 Hz, it is almost impossible to measure the pulse duration with the cross-correlation frequency-resolved optical gating (XFROG) method. The bandwidth and pulse duration of the 800-nm driving laser after focal lens are about 35 nm and about 30 fs, respectively. Therefore, the driving laser is almost Fourier-transform-limited. The bandwidth of the 29th harmonic was about 0.19 nm. According the previous work by J. Mauritsson et al. [19], the pulse duration of the 29th harmonic was estimated to be about 10–15 fs, which is normal when there is no additional pulse compression step.

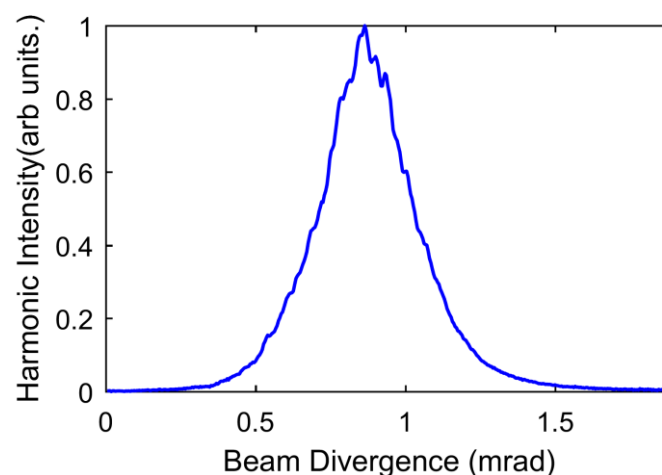


Figure 4. Beam divergence of the 29th harmonic generated under the optimized phase-matching conditions.

The energy fluctuation of the fundamental laser for 900 successive pulses is 0.54% in root mean square (rms) value [16]. Due to the stability of the fundamental pulse energy, harmonic energy has a good stability. Figure 5 shows the energy fluctuation of the 29th harmonic collected 5 times in the total time of 30 mins. In the experiment, these harmonics were accumulated with 10 shots each time. The data in the optimized phase-matching condition has been collected 5 times, but the interval time was different. The total time was about 30 mins. The results shows the energy fluctuation of the 29th harmonic in about 30 mins was 9% in rms value.

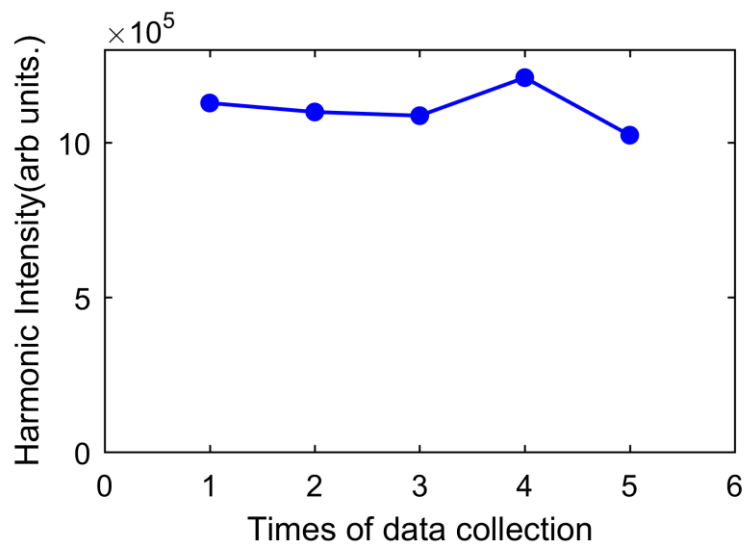


Figure 5. Energy fluctuation of the 29th harmonic collected 5 times in the total time of 30 mins.

4. Conclusions

In this paper, by using a hundred-TW-level high-power laser system, we were able to obtain a high-energy, good-quality and low-divergence harmonic pulse. The total energy in the spectral region of the 21st to 35th harmonics was estimated to be 300 nJ by a single shot. The 29th harmonic energy was estimated to be ~ 100 nJ/pulse. Therefore, the CE of the 29th harmonic was obtained to be 6×10^{-6} . High-power laser is poor in beam quality and stability, but the CE of HHG generation in this experiment is close to the results by E. Takahashi et al. [12]. The beam divergence was measured to be 0.3 mrad (FWHM). The generated soft X-ray (~ 30 nm) sources with high stable energy, good beam quality will be sent as a seed into an XEL-like amplifier with GeV electrons from LWFA to produce short-wavelength full-coherent X-ray radiation in SIOM.

Author Contributions: Experimental Design, Y.Z. and Z.Z.; HHG Experiment, L.Z., Y.Z., G.L., and Z.J.; 200-TW Laser Resources, Y.L., Y.X., and Y.L.; Supervision, Y.Z. and Z.Z.; Funding Acquisition, R.L. and Z.X.; Writing of the Original Draft Preparation, L.Z.; Writing of Review and Editing, Y.Z.

Funding: This research was funded by the National Natural Science Foundation of China (grant No. 11574332, No. 61690223, No. 11774363, No. 11561121002, No. 61521093, No. 11127901 and No. 11227902), the Strategic Priority Research Program of the Chinese Academy of Sciences (grant No. XDB16), and the Chinese Academy Sciences (CAS) Youth Innovation Promotion Association.

Acknowledgments: We thank the Beijing Synchrotron Radiation Facility (BSRF) for calibrating the XUV photodiode detector.

Conflicts of Interest: The authors declare no conflicts of interest.

References

1. Ditmire, T.; Gumbrell, E.T.; Smith, R.A.; Tisch, J.W.; Meyerhofer, D.D.; Hutchinson, M.H. Spatial coherence measurement of soft x-ray radiation produced by high order harmonic generation. *Phys. Rev. Lett.* **1996**, *77*, 4756–4759. [[CrossRef](#)] [[PubMed](#)]
2. Bellini, M.; Lynga, C.; Tozzi, A.; Gaarde, M.B.; Hansch, T.W.; L’Huillier, A.; Wahlstrom, C.G. Temporal coherence of ultrashort high-order harmonic pulses. *Phys. Rev. Lett.* **1998**, *81*, 297–300. [[CrossRef](#)]
3. Salieres, P.; L’Huillier, A.; Lewenstein, M. Coherence control of high-order harmonics. *Phys. Rev. Lett.* **1995**, *74*, 3776–3779. [[CrossRef](#)] [[PubMed](#)]
4. Lewenstein, M.; Balcou, P.; Ivanov, M.Y.; L’Huillier, A.; Corkum, P.B. Theory of high-harmonic generation by low-frequency laser fields. *Phys. Rev. A* **1994**, *49*, 2117–2132. [[CrossRef](#)] [[PubMed](#)]

5. Ishikawa, K.; Midorikawa, K. Two-photon ionization of he+ as a nonlinear optical effect in the soft-x-ray region. *Phys. Rev. A* **2002**, *65*, 043405. [[CrossRef](#)]
6. Mairesse, Y.; de Bohan, A.; Frasinski, L.J.; Merdji, H.; Dinu, L.C.; Monchicourt, P.; Breger, P.; Kovacev, M.; Taieb, R.; Carre, B.; et al. Attosecond synchronization of high-harmonic soft x-rays. *Science* **2003**, *302*, 1540–1543. [[CrossRef](#)] [[PubMed](#)]
7. Krasnoperova, A.A.; Rippstein, R.; Flamholz, A.; Kratchmer, E.; Wind, S.; Brooks, C.; Lercel, M. Imaging capabilities of proximity x-ray lithography at 70 nm ground rules. *Proc. SPIE* **1999**, *3676*, 24–39.
8. Zeitoun, P.; Faivre, G.; Sebban, S.; Mocek, T.; Hallou, A.; Fajardo, M.; Aubert, D.; Balcou, P.; Burgy, F.; Douillet, D.; et al. A high-intensity highly coherent soft x-ray femtosecond laser seeded by a high harmonic beam. *Nature* **2004**, *431*, 426–429. [[CrossRef](#)] [[PubMed](#)]
9. Lambert, G.; Hara, T.; Garzella, D.; Tanikawa, T.; Labat, M.; Carre, B.; Kitamura, H.; Shintake, T.; Bougeard, M.; Inoue, S.; et al. Injection of harmonics generated in gas in a free-electron laser providing intense and coherent extreme-ultraviolet light. *Nat. Phys.* **2008**, *4*, 296–300. [[CrossRef](#)]
10. Ditmire, T.; Crane, J.K.; Nguyen, H.; DaSilva, L.B.; Perry, M.D. Energy-yield and conversion-efficiency measurements of high-order harmonic radiation. *Phys. Rev. A* **1995**, *51*, R902–R905. [[CrossRef](#)] [[PubMed](#)]
11. Constant, E.; Garzella, D.; Breger, P.; Mevel, E.; Dorrer, C.; Le Blanc, C.; Salin, F.; Agostini, P. Optimizing high harmonic generation in absorbing gases: Model and experiment. *Phys. Rev. Lett.* **1999**, *82*, 1668–1671. [[CrossRef](#)]
12. Takahashi, E.; Nabekawa, Y.; Otsuka, T.; Obara, M.; Midorikawa, K. Generation of highly coherent submicrojoule soft x rays by high-order harmonics. *Phys. Rev. A* **2002**, *66*, 021802. [[CrossRef](#)]
13. Takahashi, E.; Nabekawa, Y.; Midorikawa, K. Generation of 10- μ j coherent extreme-ultraviolet light by use of high-order harmonics. *Opt. Lett.* **2002**, *27*, 1920–1922. [[CrossRef](#)] [[PubMed](#)]
14. Takahashi, E.J.; Nabekawa, Y.; Midorikawa, K. Low-divergence coherent soft x-ray source at 13 nm by high-order harmonics. *Appl. Phys. Lett.* **2004**, *84*, 4–6. [[CrossRef](#)]
15. Erny, C.; Mansten, E.; Gisselbrecht, M.; Schwenke, J.; Rakowski, R.; He, X.; Gaarde, M.B.; Werin, S.; L’Huillier, A. Metrology of high-order harmonics for free-electron laser seeding. *New J. Phys.* **2011**, *13*, 073035. [[CrossRef](#)]
16. Xu, Y.; Lu, J.; Li, W.K.; Wu, F.X.; Li, Y.Y.; Wang, C.; Li, Z.Y.; Lu, X.M.; Liu, Y.Q.; Leng, Y.X.; et al. A stable 200tw/1hz ti: Sapphire laser for driving full coherent xfel. *Opt. Laser Technol.* **2016**, *79*, 141–145. [[CrossRef](#)]
17. Wang, W.T.; Li, W.T.; Liu, J.S.; Zhang, Z.J.; Qi, R.; Yu, C.H.; Liu, J.Q.; Fang, M.; Qin, Z.Y.; Wang, C.; et al. High-brightness high-energy electron beams from a laser wakefield accelerator via energy chirp control. *Phys. Rev. Lett.* **2016**, *117*, 124801. [[CrossRef](#)] [[PubMed](#)]
18. Takahashi, E.J.; Hasegawa, H.; Nabekawa, Y.; Midorikawa, K. High-throughput, high-damage-threshold broadband beam splitter for high-order harmonics in the extreme-ultraviolet region. *Opt. Lett.* **2004**, *29*, 507–509. [[CrossRef](#)] [[PubMed](#)]
19. Mauritsson, J.; Johnsson, P.; López-Martens, R.; Varjú, K.; Kornelis, W.; Biegert, J.; Keller, U.; Gaarde, M.B.; Schafer, K.J.; L’Huillier, A. Measurement and control of the frequency chirp rate of high-order harmonic pulses. *Phys. Rev. A* **2004**, *70*, 021801. [[CrossRef](#)]

